

Cite this: *Phys. Chem. Chem. Phys.*,  
2014, 16, 1930

## Non-equivalent conformations of D-amino acid oxidase dimer from porcine kidney between the two subunits. Molecular dynamics simulation and photoinduced electron transfer†

Arthit Nueangaudom,<sup>a</sup> Kiattisak Lugsanangarm,<sup>a</sup> Somsak Pianwanit,<sup>\*a</sup> Sirirat Kokpol,<sup>a</sup> Nadtanet Nunthaboot<sup>b</sup> and Fumio Tanaka<sup>‡, \*ac</sup>

The structural difference between two subunits of D-amino acid oxidase dimer from porcine kidney was studied by molecular dynamics simulation (MDS) and rate of photoinduced electron transfer (ET) from aromatic amino acids as tyrosines (Tyr) and tryptophanes (Trp) to the excited isoalloxazine (Iso\*). The donor–acceptor distances ( $R_c$ ) between isoalloxazine (Iso) and the donors were shortest in Tyr224 (0.74 nm) in Sub A at 10 °C (Sub A10), in Tyr224 (0.79 nm) in Sub B at 10 °C (Sub B10), in Tyr228 (0.85 nm) in Sub A at 30 °C (Sub A30), and in Tyr224 (0.72 nm) in Sub B at 30 °C (Sub B30). The  $R_c$ s were mostly shorter in the dimer than those in the monomer. Hydrogen bonding (H-bond) pairs between Iso and surrounding amino acids varied with the subunit and temperature. O2 of the Iso ring formed an H-bond exclusively with Thr317OG1 (side chain) in both Sub A10 and Sub A30, while it formed with Gly315N (peptide), Leu316N and Thr317N in Sub B10 and Sub B30. N3H of Iso formed an H-bond with Leu51O (peptide) in Sub A10 and Sub A30, but not in Sub B10 and Sub B30. Electron affinity of Iso\* was appreciably lower in Sub A10 compared to Sub B10, while it was opposite at 30 °C. ET rate to Iso\* was fastest from Tyr224 in Sub A10, while it was fastest from Tyr314 in Sub B10. The ET rate was fastest from Tyr314 in Sub A30, while it was fastest from Tyr224 in Sub B30. The greater ET rates in the dimer as compared to those in the monomer were elucidated with shorter  $R_c$  in the dimer as compared to the monomer. The static dielectric constants inside the subunits and the static dielectric constant between Iso and Tyr224 or Tyr228 were not different appreciably. A few water molecules and sometimes an amino acid were located between Iso and Tyr224, which may be the reason why the dielectric constant of the entire subunits did not differ from that between Iso and Tyr224.

Received 9th September 2013,  
Accepted 29th October 2013

DOI: 10.1039/c3cp53826e

[www.rsc.org/pccp](http://www.rsc.org/pccp)

### I. Introduction

D-Amino acid oxidase (DAAO) is a peroxisomal enzyme containing flavin adenine dinucleotide (FAD) as a cofactor which exists in a wide range of species from yeasts to humans. Its function is to oxidize D-amino acids to the corresponding imino acids, producing ammonia and hydrogen peroxide. A number of review articles have been reported on DAAO from porcine kidney<sup>1,2</sup> from

yeast to human,<sup>3</sup> and from human.<sup>4,5</sup> Recently, mammalian DAAO has been demonstrated to connect with the brain D-serine metabolism and to the regulation of the glutamatergic neurotransmission.<sup>6,7</sup> Various novel inhibitors to human DAAO have been found using the *in silico* screening technique.<sup>8</sup>

DAAO from porcine kidney is in a monomer ( $M_w$  39 kDa) – dimer equilibrium state at relatively low concentrations,<sup>9–12</sup> and may be in a dimer–tetramer equilibrium at higher concentrations.<sup>13–15</sup> The crystal structures of DAAO from porcine kidney were determined by Miura *et al.*<sup>16</sup> and Mattevi *et al.*<sup>17</sup> A temperature-induced conformational change of the DAAO has been reported by many workers.<sup>18–23</sup> The fluorescence lifetime of the dimer is *ca.* 40 ps while that of the monomer is 160 ps, which suggests that the structure near to Iso in the dimer is quite different from the monomer.<sup>21–23</sup>

The fluorescence of flavins in many flavoproteins is strongly quenched, which is ascribed to photoinduced electron transfer (ET) from tryptophanes (Trp) and/or tyrosines (Tyr) to the excited

<sup>a</sup> Department of Chemistry, Faculty of Science, Chulalongkorn University, 254 Phayathai Road, Bangkok 10330, Thailand. E-mail: Somsak.t@chula.ac.th

<sup>b</sup> Department of Chemistry, Faculty of Science, Mahasarakham University, Mahasarakham 44150, Thailand

<sup>c</sup> Division of Laser Bio-science, Institute for Laser Technology, Utsubo-Honmachi, 1-8-4, Nishiku, Osaka 550-0004, Japan

† Electronic supplementary information (ESI) available. See DOI: 10.1039/c3cp53826e

‡ Division of Laser Biochemistry, Institute for Laser Technology, Utsubo-Honmachi, 1-8-4, Nishiku, Osaka 550-0004, Japan. E-mail: fumio.tanaka@yahoo.com

isoalloxazine ( $\text{Iso}^*$ ).<sup>24–26</sup> Ultrafast fluorescence dynamics of some flavoproteins in the time domain of femtoseconds–picoseconds have been studied by a fluorescence up-conversion technique.<sup>27–31</sup> The ultrafast fluorescence dynamics of some flavoproteins have been analyzed with the protein structures obtained by molecular dynamics simulation (MDS) and an electron transfer theory.<sup>32–35</sup>

The structural basis for temperature-induced transition of DAAO monomer from porcine kidney has been analyzed with this method. The conformational change was characterized from the ET rates from Tyr224, Tyr228 and Tyr314 to the  $\text{Iso}^*$ .<sup>36</sup> The ultrafast fluorescence dynamics of DAAO–benzoate complex has also been analyzed with MDS snapshots and Kikitani and Mataga (KM) theory.<sup>37</sup> In the present work we have demonstrated by means of the MDS structures and ET analysis that the structure of DAAO dimer is quite different between the two subunits, and provide the structural basis of the conformational difference between dimer and monomer.

## II. Method of analysis

### MDS calculations

All MDS were performed using the Amber10 suite program.<sup>38</sup> The starting structure from the X-ray structure of the

DAAO–benzoate complex dimer (PDB code 1VE9)<sup>16</sup> was removing two benzoate molecules from each subunit. The protein was added hydrogen atoms for all missing hydrogen atoms using LEaP module of Amber10.<sup>38</sup> Subsequently, the protein complex was solvated with a cubic box of 7395 TIP3P water molecules and eight sodium counterions added for the electroneutrality of the system. The parm99 force field<sup>39</sup> was used to generate the protein topology and the restrained electrostatic potential (RESP)<sup>40</sup> charges was used for the FAD. The simulated system was minimized with 2000 steps of the steepest descent followed by 3000 steps of conjugate gradient of energy minimization. Afterwards, both systems were heated from 0 to 283 K or from 0 to 303 K (for the 10 and 30 °C MDS, respectively) over 100 ps and were further equilibrated under periodic boundary conditions at 283 and 303 K. The systems were set up under the isobaric-isothermal ensemble with a constant pressure of 1 atm and constant temperature of either 283 or 303 K. The electrostatic interactions were corrected by the Particle Mesh Ewald method.<sup>41</sup> The SHAKE algorithm<sup>42</sup> was employed to constrain all bonds involving hydrogen atoms. MDS based calculations were performed with time steps of 2 fs and a cutoff distance of 1 nm was employed for non-bonded pair interactions. The stability of the system was checked by investigating the convergence of the energies, temperature, pressure and global root mean square deviation of the system. The equilibrium was found to be attained after 20 ns of the MDS calculation, by

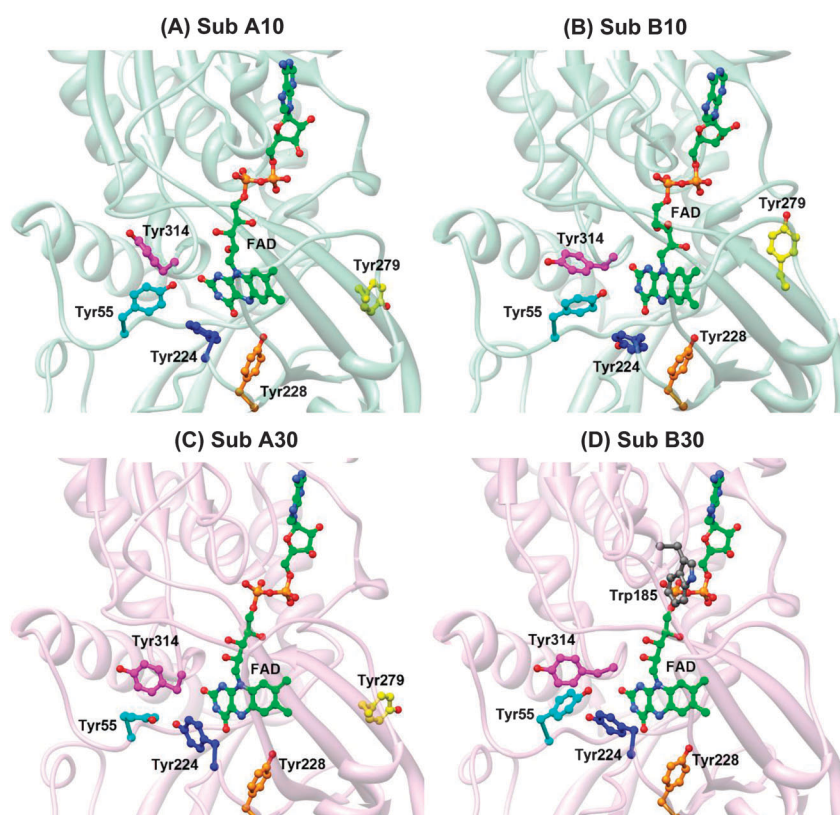


**Fig. 1** Local structure of FAD binding site in DAAO obtained by MDS. The five fastest ET donors are illustrated with stick model, together with FAD. Sub A10 and Sub B10 denote subunits of A and B at 10 °C, and Sub A30 and Sub B30 denote subunits of A and B at 30 °C. MDS calculations were performed independently both at 10 °C and 30 °C.

monitoring these quantities. Then the calculation was continued for up to further 30 ns, and data from the last 5 ns were used for the analyses.

### ET theory

The original Marcus theory<sup>43,44</sup> has been modified in various ways.<sup>45–48</sup> In the present analysis, KM theory<sup>47</sup> was used, because it is applicable for non-adiabatic ET process in addition to adiabatic ET process, and has been found to give satisfactory results for both static<sup>31,49,50</sup> and dynamic ET analyses.<sup>32–37</sup> The ET rate described by the KM model is expressed by eqn (1).

$$k_{\text{ET}}^{\text{jk}}(T) = \frac{\nu_0^q}{1 + \exp\{\beta^q(R_{\text{jk}} - R_0^q)\}} \sqrt{\frac{k_B T}{4\pi\lambda_{\text{jk}}^q}} \\ \times \exp\left[-\frac{\left\{\Delta G_k^0(T) - e^2/\epsilon_0^{\text{pk}} R_{\text{jk}} + \lambda_{\text{jk}}^q + E_{\text{Net}}^k(j)\right\}^2}{4\lambda_{\text{jk}}^q k_B T}\right] \quad (1)$$

Here  $k_{\text{ET}}^{\text{jk}}(T)$  is the ET rate from a donor j to the Iso\* in subunit k (k = Sub A or Sub B) at temperature T (°C), and q denotes Trp or Tyr.  $\nu_0^q$  is an adiabatic frequency,  $\beta^q$  is the ET process coefficient.  $R_{\text{jk}}$  and  $R_0^q$  are the donor j–Iso distance in subunit k and its critical distance for the ET process, respectively.  $R_{\text{jk}}$  is

expressed as a center-to-center distance ( $R_c$ ) rather than as an edge-to-edge ( $R_e$ ) distance.<sup>32–37</sup> The ET process is adiabatic when  $R_{\text{jk}} < R_0^q$ , and non-adiabatic when  $R_{\text{jk}} > R_0^q$ .  $T$  in the right hand sides of eqn (1) is temperature expressed in K unit. The term,  $-e^2/\epsilon_0^{\text{pk}} R_{\text{jk}}$ , in eqn (1) is electrostatic (ES) energy between Iso anion and a donor cation. The static dielectric constant ( $\epsilon_0^{\text{pk}}$ ) is discussed below eqn (2). The terms  $k_B$  and  $e$  are the Boltzmann constant and electron charge, respectively.  $E_{\text{Net}}^k(j)$  is the Net ES energy of the donor j in subunit k, which is described later. The porcine kidney DAO monomer contains 10 Trp and 14 Tyr residues. In the present work the ET rates from all of these aromatic amino acids to Iso\* were taken into account for the analysis.

$\lambda_{\text{jk}}^q$  is the solvent reorganization energy<sup>43,44</sup> of the ET donor q j, and is expressed as eqn (2).

$$\lambda_{\text{jk}}^q = e^2 \left( \frac{1}{2a_{\text{Iso}}} + \frac{1}{2a_q} - \frac{1}{R_{\text{jk}}} \right) \left( \frac{1}{\epsilon_\infty} - \frac{1}{\epsilon_0^{\text{pk}}} \right) \quad (2)$$

where  $a_{\text{Iso}}$  and  $a_q$  are the radii of Iso and Trp or Tyr, with these reactants being assumed to be spherical, and  $\epsilon_\infty$  is optical dielectric constant, and  $\epsilon_0^{\text{pk}}$  static dielectric constant of subunit k. It was assumed that for Tyr224 and Tyr228  $\epsilon_0^{\text{pA}}(\text{Sub A}) = \epsilon_0^{\text{pB}}(\text{Sub B}) = \epsilon_0^{\text{DA}}$ , where  $\epsilon_0^{\text{DA}}$  is static dielectric constant between the donor and Iso, because these donor–acceptor distances were always much shorter than 1 nm, and for the other donors

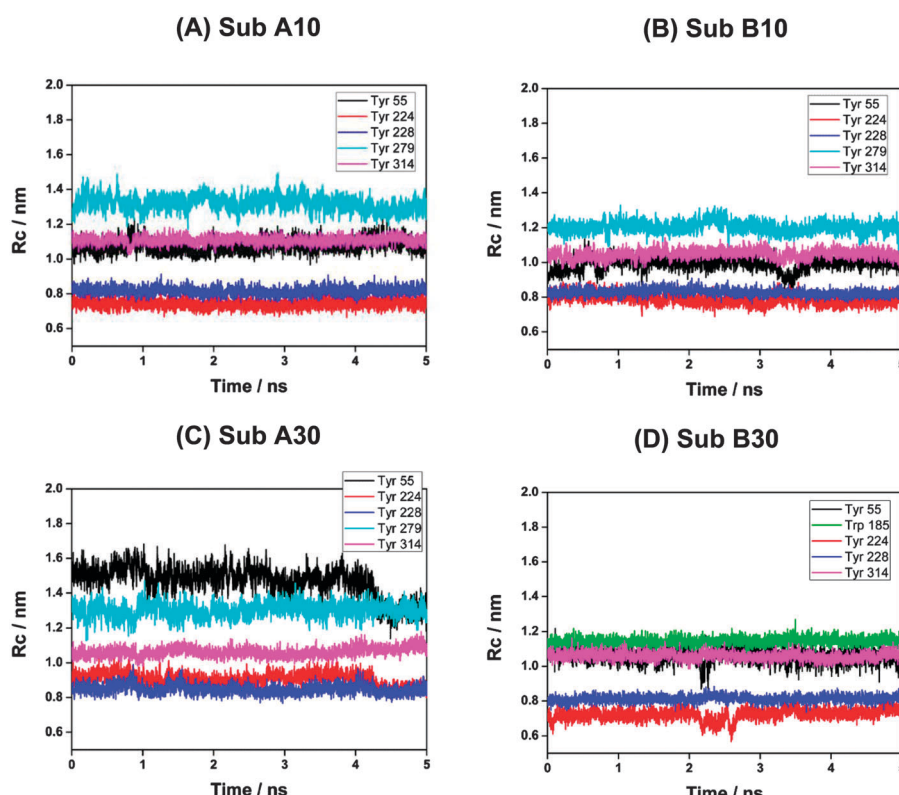
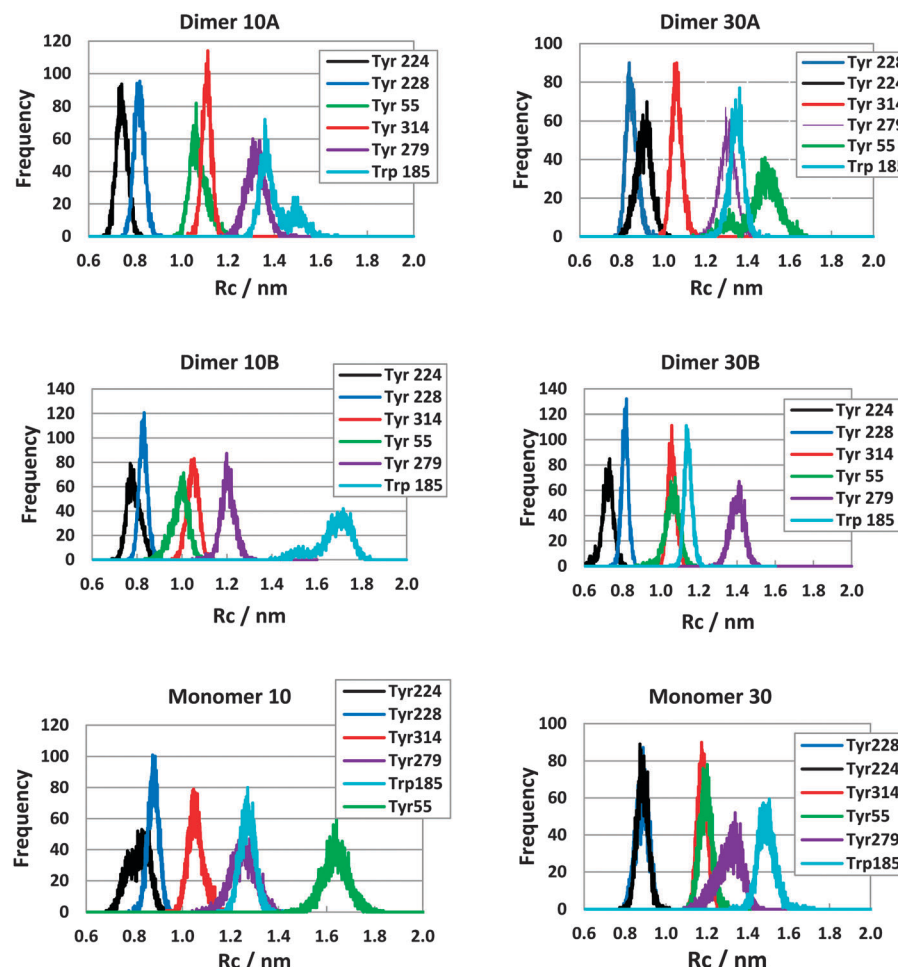


Fig. 2 Time evolution of the donor–acceptor distance. ET donors are aromatic amino acids indicated in the insets, and acceptor is Iso\*. The distances are expressed with the center-to-center distance ( $R_c$ ). Sub A10 and Sub B10 denote subunits of A and B at 10 °C, and Sub A30 and Sub B30 denote subunits of A and B at 30 °C. MDS calculations were performed independently both at 10 and 30 °C.



**Fig. 3** The distribution of the donor–acceptor distance. The distances are expressed with center-to-center distance ( $R_c$ ). 10A and 10B denote Sub A and Sub B at 10 °C, and 30A and 30B, Sub A and Sub B at 30 °C. Sub A and Sub B denote subunits A and B. Time evolutions of the distances are shown in Fig. 2. MDS were performed at 10 °C and 30 °C. The distributions for monomers are also illustrated for comparison.<sup>36</sup>

$\varepsilon_0^{\text{PA}}(\text{Sub A}) = \varepsilon_0^{\text{A}}$ ,  $\varepsilon_0^{\text{PB}}(\text{Sub B}) = \varepsilon_0^{\text{B}}$ . The optical dielectric constant used was 2.0. The radii of Iso ( $a_{\text{Iso}}$ ), Trp ( $a_{\text{Trp}}$ ) and Tyr ( $a_{\text{Tyr}}$ ) were

those previously determined<sup>32–35</sup> to be 0.224, 0.196 and 0.173 nm, respectively.

**Table 1** ET donor–acceptor distance<sup>a</sup>

DAAO	T (°C)	Subunit	Donor <sup>b</sup> ( $R_c$ /nm)					
Dimer	10	A	Tyr224 (0.74)	Tyr228 (0.82)	Tyr55 (1.07)	Tyr314 (1.11)	Tyr279 (1.32)	
	10	B	Tyr224 (0.79)	Tyr228 (0.83)	Tyr55 (0.99)	Tyr314 (1.05)	Tyr279 (1.20)	
	30	A	Tyr228 (0.85)	Tyr224 (0.90)	Tyr314 (1.06)	Tyr279 (1.30)	Tyr55 (1.47)	
	30	B	Tyr224 (0.72)	Tyr228 (0.81)	Tyr314 (1.06)	Tyr55 (1.06)	Trp185 (1.14)	
Monomer <sup>c</sup>	10		Tyr224 (0.82)	Tyr228 (0.88)	Tyr314 (1.06)	Trp185 (1.27)	Tyr55 (1.64)	
	30		Tyr224 (0.88)	Tyr228 (0.88)	Tyr314 (1.18)	Tyr55 (1.20)	Trp185 (1.49)	
Benzoate complex Monomer <sup>d</sup>	20		Tyr228 (0.81)	Tyr224 (0.97)	Tyr314 (1.07)	Tyr279 (1.24)	Tyr74 (1.80)	Benzoate (0.61)

<sup>a</sup> Mean center-to-center distances ( $R_c$ ) are listed over 5000 snapshots. <sup>b</sup> Five shortest distances between Iso and the aromatic amino acids or benzoate are listed in order from shorter to longer distances. <sup>c</sup> Data taken from ref. 36. <sup>d</sup> Data taken from ref. 37.

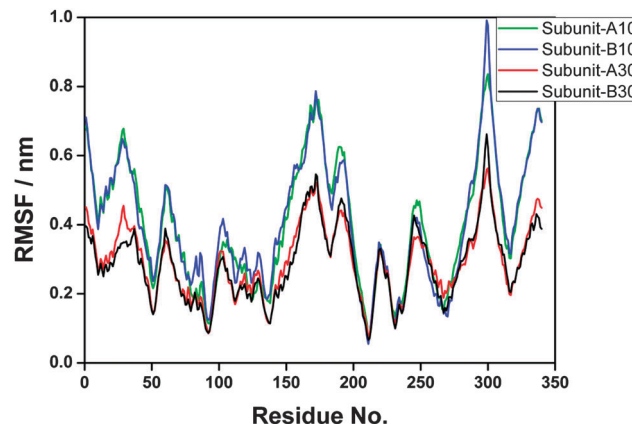


**Fig. 4** RMSF of DAAO dimer. RMSF of Sub A at 10 °C is illustrated with green line, Sub B at 10 °C with blue line, Sub A at 30 °C with red line, Sub B at 30 °C with a black line. Maximum RMSFs were obtained at Ser300 in Sub A10, Gly299 in Sub B10, Ser300 in Sub A30 and Gly299 in Sub B30. Next highest regions were around the residue No. 170. The peak amino acids in this region were Arg172 in Sub A10 and in Sub B10, and Gly173 in Sub A30 and Arg172 in Sub B30.

The standard free energy change was expressed with the ionization potential of the ET donor,  $E_{\text{IP}}^q$ , as eqn (3).

$$\Delta G_k^0(T) = E_{\text{IP}}^q - G_k^0(T) \quad (3)$$

where  $G_k^0(T)$  is the standard Gibbs energy related to the electron affinity of Iso\* in subunit k at temperature T. The values of  $E_{\text{IP}}^q$  for Trp and Tyr were 7.2 and 8.0 eV, respectively.<sup>51</sup>

### Electrostatic energy in DAAO dimer

Protein systems contain many ionic groups, which may influence the ET rate. The porcine kidney DAAO contains Iso as the ET acceptor, and 10 Trp residues and 14 Tyr residues per subunit as potential ET donors. The FAD cofactor in DAAO has two negative charges at the pyrophosphate, whilst DAAO itself contains 22 Glu, 13 Asp, 12 Lys and 21 Arg residues per subunit. Therefore total numbers of ionic groups are double of those in one subunit. The ES energy between the Iso anion or donor cation j and all other ionic groups in subunit k (Sub A or Sub B) is expressed by eqn (4).

$$E_k(j) = \sum_{i=1}^{44} \frac{C_j C_{\text{Glu}}}{\epsilon_0^{\text{pk}} R_j(\text{Glu}-i)} + \sum_{i=1}^{26} \frac{C_j C_{\text{Asp}}}{\epsilon_0^{\text{pk}} R_j(\text{Asp}-i)} \\ + \sum_{i=1}^{24} \frac{C_j C_{\text{Lys}}}{\epsilon_0^{\text{pk}} R_j(\text{Lys}-i)} + \sum_{i=1}^{42} \frac{C_j C_{\text{Arg}}}{\epsilon_0^{\text{pk}} R_j(\text{Arg}-i)} + \sum_{i=1}^8 \frac{C_j C_P}{\epsilon_0^{\text{pk}} R_j(\text{P}-i)} \quad (4)$$

Here  $j = 0$  for the Iso anion in subunit k, 1–10 for the Trp cations in Sub A and 11–20 for Trp in Sub B, 21–34 for the Tyr cations in Sub A, and 35–48 for Tyr cations in Sub B.  $C_j$  is the charge of the aromatic ionic species j, that is,  $-e$  for  $j = 0$  and  $+e$  for  $j = 1$  to 48.  $C_{\text{Glu}}(-e)$ ,  $C_{\text{Asp}}(-e)$ ,  $C_{\text{Lys}}(+e)$ , and  $C_{\text{Arg}}(+e)$  are the charges of the Glu, Asp, Lys and Arg residues, respectively. FAD contains 2 phosphate atoms, each of which binds 2 oxygen atoms. It was assumed that the charge of each oxygen atom is  $C_P = -0.5e$ , though total charge of four oxygen atoms is  $-2e$ . We also assumed that these groups are all in an ionic state in solution. The distances between the aromatic ionic species j

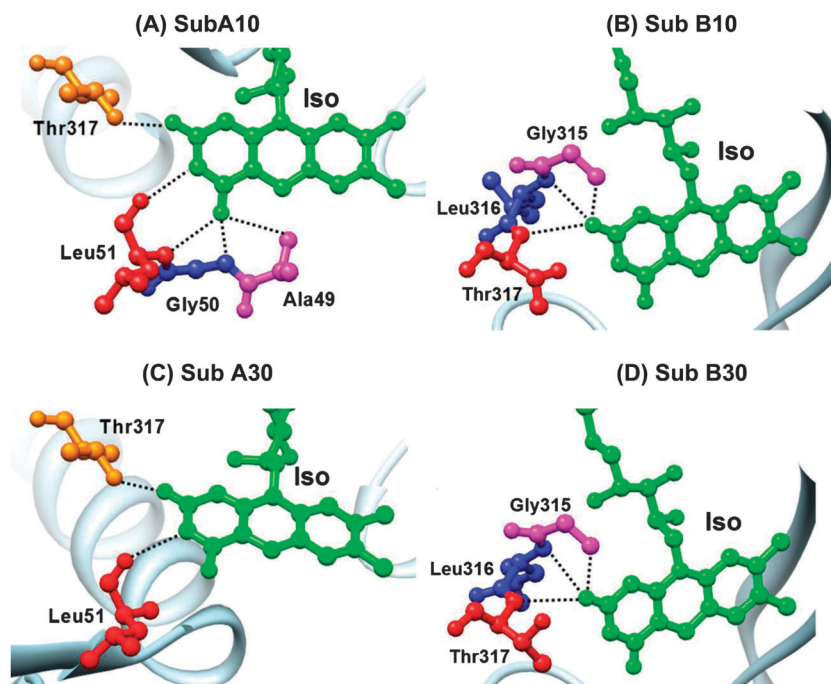


**Fig. 5** H-bond structure between the Iso ring and the nearby amino acids. Sub A10 and Sub B10 denote subunits of A and B at 10 °C, and Sub A30 and Sub B30 denote subunits of A and B at 30 °C. The H-bond distances are listed in Table 2.

Table 2 Comparison of H-bond distances among tow subunits in the dimer and in the monomer

Iso ring <sup>b</sup>	Amino acid	Distance <sup>a</sup> (nm)		Dimer Sub B		Monomer <sup>c</sup>	
		10 °C	30 °C	10 °C	30 °C	10 °C	30 °C
N3H	Leu51 O	0.29	0.29	—	—	—	—
N5	Ala49 N	—	—	—	—	—	—
O2	Gly315 N	—	—	0.29	0.29	—	—
	Leu316 N	—	—	0.28	0.28	—	0.29
	Thr317 N	—	—	0.29	0.29	—	—
O4	Thr317 OG1	0.28	0.28	—	—	—	—
	Ala49 N	—	—	—	—	—	—
	Gly50 N	0.29	—	—	—	0.29	0.29
	Leu51 N	0.29	—	—	—	—	—

<sup>a</sup> Atomic notations in Iso are as indicated in Chart 1. <sup>b</sup> Criteria for H-bond distance was taken as within 0.3 nm. <sup>c</sup> Data taken from ref. 36, and listed the distances shorter than 0.3 nm.

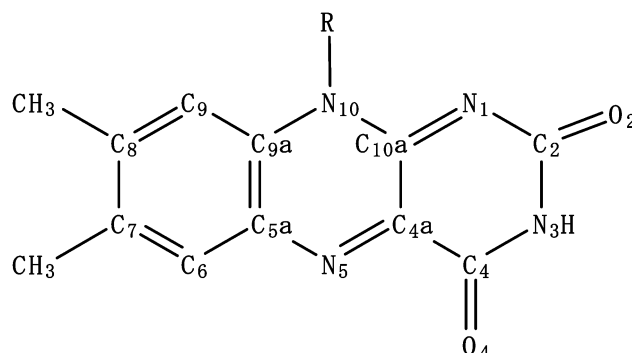


Chart 1 Chemical structure and atom notations of Iso.

and the *i*th Glu (*i* = 1–44) are denoted as  $R_j(\text{Glu-}i)$ , whilst the distances between the aromatic ionic species *j* and the *i*th Asp (*i* = 1–26) are denoted as  $R_j(\text{Asp-}i)$ , and so on for the each amino acid residue.

$E_{\text{Net}}^k(j)$  in eqn (1) was then expressed as eqn (5).

$$E_{\text{Net}}^k(j) = E_k(0) + E_k(j) \quad (5)$$

Here *j* is from 1 to 48, and represents the *j*th ET donor, as described above.

### Determination of the ET parameters

The observed fluorescence lifetimes of the porcine kidney DAO monomer are reported to be  $\tau_{\text{obs}}^{10} = 44.2$  ps at 10 °C and  $\tau_{\text{obs}}^{30} = 37.7$  ps at 30 °C.<sup>23</sup> The calculated lifetimes of subunit k at temperature (*T*) were given by eqn (6).

$$\tau_{\text{Calc.}}^{\text{Tk}} = \frac{1}{\sum_{j=1}^{48} k_{\text{ET}}^{jk}(T)} \quad (6)$$

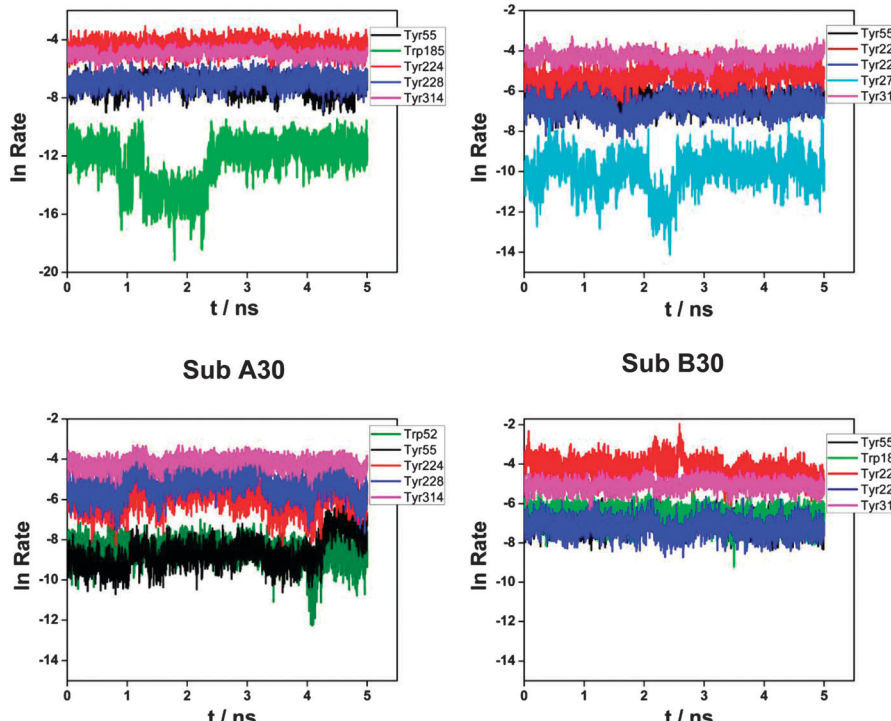
The fluorescent lifetimes were expressed in unit of ps. In the present work the physical quantities related to the electronic coupling term ( $\nu_0^g$ ,  $\beta^q$  and  $R_0^g$ ) for Trp and Tyr were taken from those reported for the flavin mononucleotide binding proteins,<sup>33</sup> which were assumed to be independent of temperature within the temperature range (10–30 °C) as in previous works.<sup>36,37</sup> On the contrary, the free energy,  $G_k^0(T)$ , related to the electron affinity of Iso\* was assumed to be both temperature- and subunit-dependent, because  $G_k^0(T)$  is modified with the hydrogen bonding (H-bond) structure.<sup>36,37</sup> The unknown ET parameters were  $G_A^0(10)$ ,  $G_B^0(10)$ ,  $G_A^0(30)$  and  $G_B^0(30)$  in eqn (3), and  $\varepsilon_0^A$ ,  $\varepsilon_0^B$  and  $\varepsilon_0^{\text{DA}}$  which were assumed to be independent of temperature.<sup>36,37</sup> These ET parameters were determined so as to obtain the minimum value of  $\chi^2$ , as given by eqn (7).

Table 3 Best-fit ET parameter<sup>a</sup>

<i>T</i> (°C)	Subunit	$\varepsilon_0^{\text{pk}} b$	$G_k^0(T)^c$ (eV)	$\Delta G_k^0(T)^d$ (eV)		$\tau$ (ps)		Chi-sq. <sup>g</sup>
				(Trp)	(Tyr)	Obs <sup>e</sup>	Calc. <sup>f</sup>	
10	Sub A	5.79	8.16	-1.41	-0.607	44.2	44.2	$3.22 \times 10^{-28}$
	Sub B	5.82	8.54	-1.34	-0.536	—	—	$7.47 \times 10^{-28}$
	Monomer <sup>h</sup>	5.88	8.69	-1.49	-0.69	228	228	—
30	Sub A	5.79	8.73	-1.53	-0.736	37.7	37.7	$1.10 \times 10^{-25}$
	Sub B	5.82	8.48	-1.28	-0.481	—	—	$2.16 \times 10^{-28}$
	Monomer <sup>h</sup>	5.89	8.51	-1.31	-0.48	182	182	—

<sup>a</sup> The reported values of ET parameters were used for the electronic coupling term<sup>33</sup> ( $\nu_0^{\text{Trp}} = 1016$  ps<sup>-1</sup>,  $\nu_0^{\text{Tyr}} = 197$  ps<sup>-1</sup>,  $\beta^{\text{Trp}} = 21.0$  nm<sup>-1</sup>,  $\beta^{\text{Tyr}} = 6.25$  nm<sup>-1</sup>,  $R_0^{\text{Trp}} = 0.663$  nm,  $R_0^{\text{Tyr}} = 0.499$  nm). The optical dielectric constant used was 2 as in the previous works.<sup>32–37</sup> <sup>b</sup> Static dielectric constants inside Sub A ( $\varepsilon_0^A$ ) and inside Sub B ( $\varepsilon_0^B$ ), which were assumed to be temperature-independent.<sup>36,37</sup> <sup>c</sup> Temperature dependent standard free energy gap, given by eqn (3) in text. <sup>d</sup> Temperature-dependent electron affinity of Iso\*. <sup>e</sup> Reported fluorescence lifetimes.<sup>23</sup> The lifetimes of Sub A and Sub B was not experimentally resolved. <sup>f</sup> Calculated lifetimes. <sup>g</sup> Chi-square between the observed and calculated lifetimes given by eqn (7) in text. Total Chi-square was  $2.8 \times 10^{-26}$ . <sup>h</sup> ET parameters for monomer were taken from the reported work for comparison.<sup>36</sup>

### Sub A10    Sub B10



**Fig. 6** Time evolution of ET rate from aromatic amino acids to Iso\*. Insets show the five donors with fast ET rates. Mean ET rates over 5000 snapshots with 1 ps intervals are listed in Table 3.

**Table 4** Physical quantity related to ET rate<sup>a</sup>

Dimer subunit ( <i>T</i> )	Donor	$K_{ET}^{jk}(T)^b$ (ps <sup>-1</sup> )	$E_{Net}^k(j)^c$ (eV)	$\lambda_{jk}^q d$ (eV)	$-\epsilon^2/\epsilon_0^{jk} R_{jk}^k$ (eV)	$R_c$ ratio <sup>f</sup>	Monomer <sup>g</sup>	Donor	$k_{ET}^{jk}(T)^b$ (ps <sup>-1</sup> )	$E_{Net}^k(j)^b$ (eV)
A (10)	Tyr224	$1.29 \times 10^{-2}$	0.044	1.79	-0.331	0.82	10	Tyr224	$2.27 \times 10^{-3}$	0.192
	Tyr314	$7.57 \times 10^{-3}$	-0.406	1.99	-0.224	1.06		Tyr314	$1.38 \times 10^{-3}$	-0.073
	Tyr228	$1.20 \times 10^{-3}$	0.146	1.85	-0.300	0.88		Tyr228	$5.94 \times 10^{-4}$	0.215
	Tyr55	$9.08 \times 10^{-4}$	-0.119	1.97	-0.232	0.66		Trp185	$1.15 \times 10^{-4}$	-0.249
	Trp185	$9.71 \times 10^{-6}$	-0.104	1.92	-0.178	1.10		Tyr279	$1.57 \times 10^{-5}$	0.144
B (10)	Tyr314	$1.38 \times 10^{-2}$	-0.479	1.97	-0.236	0.99	10			
	Tyr224	$5.96 \times 10^{-3}$	-0.021	1.83	-0.312	0.95				
	Tyr55	$1.54 \times 10^{-3}$	-0.161	1.94	-0.250	0.60				
	Tyr228	$1.25 \times 10^{-3}$	0.056	1.86	-0.297	0.94				
	Tyr279	$6.08 \times 10^{-5}$	-0.076	2.03	-0.206	0.96				
A (30)	Tyr314	$1.63 \times 10^{-2}$	-0.293	1.97	-0.231	0.90	30	Tyr314	$2.35 \times 10^{-3}$	-0.434
	Tyr228	$5.86 \times 10^{-3}$	0.130	1.87	-0.290	0.96		Tyr224	$1.65 \times 10^{-3}$	-0.035
	Tyr224	$3.39 \times 10^{-3}$	0.108	1.90	-0.272	1.02		Tyr55	$8.00 \times 10^{-4}$	-0.324
	Tyr55	$2.43 \times 10^{-4}$	-0.207	2.09	-0.168	1.23		Tyr228	$6.85 \times 10^{-4}$	0.051
	Trp52	$2.15 \times 10^{-4}$	-0.593	1.92	-0.178	0.96		Tyr106	$5.47 \times 10^{-6}$	-0.342
B (30)	Tyr224	$1.68 \times 10^{-2}$	-0.038	1.77	-0.340	0.82	30			
	Tyr314	$6.51 \times 10^{-3}$	-0.422	1.97	-0.234	0.90				
	Trp185	$1.43 \times 10^{-3}$	-0.465	1.85	-0.216	0.77				
	Tyr55	$9.70 \times 10^{-4}$	-0.210	1.97	-0.234	0.89				
	Tyr228	$8.30 \times 10^{-4}$	0.097	1.85	-0.302	0.92				

<sup>a</sup> Mean values are listed over 5000 snapshots. ET parameters to obtain these quantities are given in Table 3. <sup>b</sup> ET rate is given by eqn (1).

<sup>c</sup> Net ES energy is given by eqn (5). The Net ES energies were obtained in the entire protein. <sup>d</sup> Solvent reorganization energy is given by eqn (2).

<sup>e</sup> Electrostatic energy between Iso anion and a donor cation. <sup>f</sup> Ratio,  $R_c$  in dimer/ $R_c$  in monomer. <sup>g</sup> Recalculated with the data given in ref. 36 and 37.

$$\chi^2 = \frac{(\tau_{\text{Calc.}}^{10A} - \tau_{\text{Obs.}}^{10})^2}{\tau_{\text{Calc.}}^{10A}} + \frac{(\tau_{\text{Calc.}}^{10B} - \tau_{\text{Obs.}}^{10})^2}{\tau_{\text{Calc.}}^{10B}} + \frac{(\tau_{\text{Calc.}}^{30A} - \tau_{\text{Obs.}}^{30})^2}{\tau_{\text{Calc.}}^{30A}} + \frac{(\tau_{\text{Calc.}}^{30B} - \tau_{\text{Obs.}}^{30})^2}{\tau_{\text{Calc.}}^{30B}} \quad (7)$$

### III. Results

#### Local structure near Iso binding site in DAAO dimer obtained by MDS

Fig. 1 shows MDS snapshots near FAD binding sites in DAAO dimer at 10 and 30 °C. In the Figure the structures of Sub A and

Sub B are illustrated separately. Aromatic amino acids of potential ET donor are also shown in addition to FAD. Tyr224, Tyr228, Tyr55, Tyr314 and Tyr279 are five closest donors to Iso in Sub A at 10 °C (Sub A10; Fig. 1A). In Sub B10 the aromatic amino acids of five closest to Iso were the same with those in Sub A (Fig. 1B). In Sub A30 Tyr228, Tyr224, Tyr314, Tyr279 and Tyr55 were five closest donors to Iso (Fig. 1C). In Sub B30 Tyr224, Tyr228, Tyr314, Tyr55 and Trp185 were closest to Iso (Fig. 1D). Fig. 2 shows time evolutions of  $R_c$  between these aromatic amino acids and Iso. Fig. 3 shows the  $R_c$ -distributions. The distributions may be clearer to understand differences in the  $R_c$  and extent of the distance fluctuation.  $R_c$  of Tyr185 displayed double maxima in both Sub A10 at around 1.35 nm with a major distribution and 1.5 nm with a

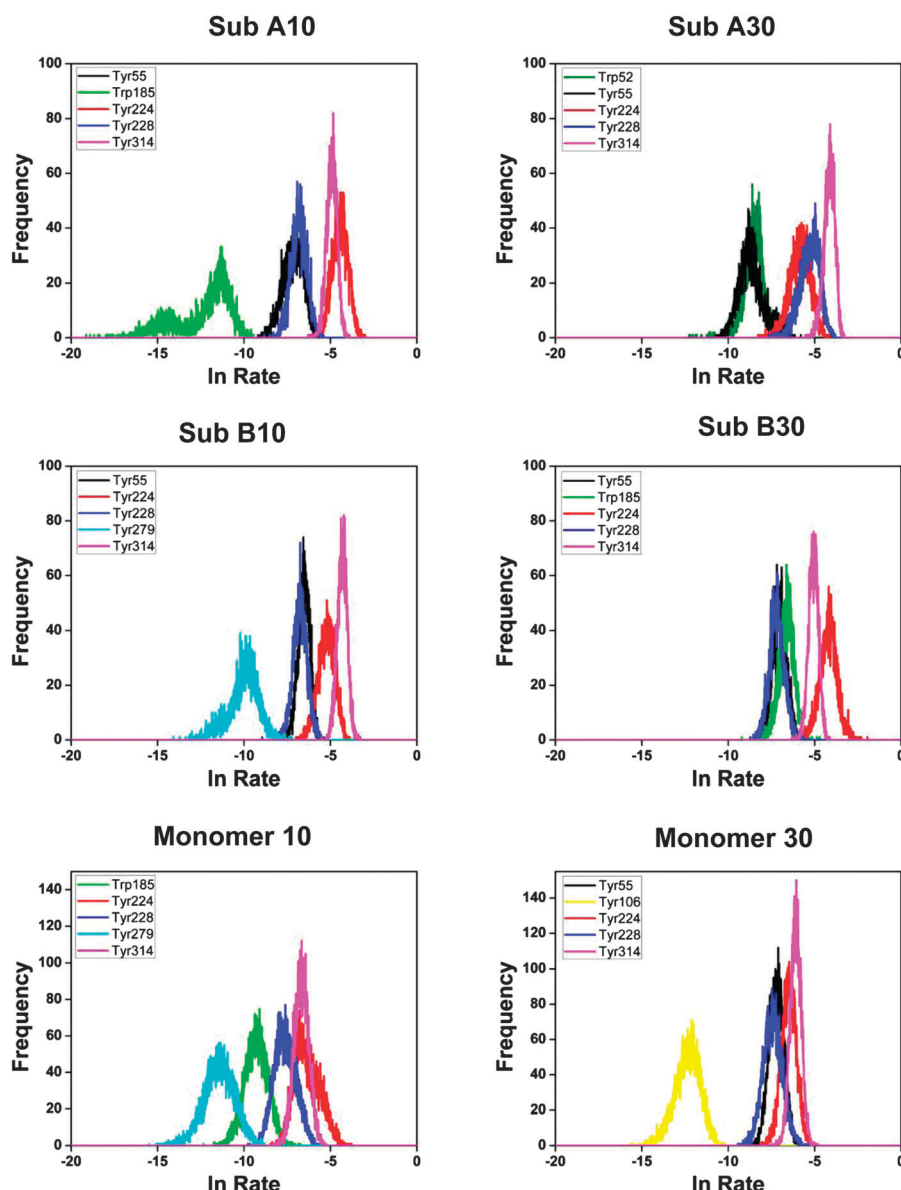


Fig. 7 Distribution of logarithmic ET rate from aromatic amino acids to Iso\*. Sub A10 and Sub B10 denote Sub A and Sub B at 10 °C in the dimer, and Sub A30 and Sub B30, Sub A and Sub B at 30 °C. Insets show amino acids with top fastest ET rates. The distributions for DAAO monomers at 10 °C (Monomer 10) and 30 °C (Monomer 30) are also shown for comparison. Kind of the amino acids are different among the six groups including monomer.

minor distribution.  $R_c$  in Sub B10 also displayed double maxima with minor distribution at around 1.5 nm and with major distribution at around 1.7 nm. The  $R_c$  of Tyr185 in monomer at 10 °C did not show such double maxima, a single peak at around 1.3 nm, which was similar to the major peak in Sub A at 10 °C. The distributions of Trp185 in dimer displayed single peaks in both Sub A and Sub B at 30 °C. The distribution of  $R_c$  in Tyr55 displayed double maxima in Sub A30, but single peak in Sub B30. The  $R_c$  at the main peak was much longer than those in Sub B30, and also in both Sub A10 and Sub B10. These results in  $R_c$  suggest that the protein conformation is quite different between Sub A and Sub B, and is appreciably modified by temperature.

Table 1 lists mean values of  $R_c$  over 5000 snapshots with 1 ps time intervals. In Sub A10 the  $R_c$  values were 0.74 nm in Tyr224, 0.82 nm in Tyr228, 1.07 nm in Tyr55, and 1.11 nm in Tyr314. In Sub B10 the  $R_c$  values were 0.79 nm in Tyr224, 0.83 nm in Tyr228, 0.99 nm in Tyr55, and 1.05 nm in Tyr314. Comparing between Sub A10 and Sub B10, the  $R_c$  values of Tyr55 and Tyr314 are a little shorter by 0.06–0.08 nm in Sub B. In Sub A30 the  $R_c$  values were 0.85 nm in Tyr228, 0.90 nm in Tyr224 and 1.06 nm in Tyr314. In Sub B30 the  $R_c$  values were 0.72 nm in Tyr224, 0.81 nm in Tyr228, 1.06 nm in Tyr55 and Tyr314. Comparing between Sub A30 and Sub B30, the  $R_c$  value of Tyr55 in Sub B were remarkably shorter by 0.41 nm than that in Sub A.

The donor–acceptor distances in the dimer were compared to those in the monomer.<sup>36</sup> Table 1 also lists the mean  $R_c$  values of the monomer. Most marked change was Tyr55 as revealed in the distance distributions. The  $R_c$  values of Tyr55 in the dimer were 1.07 nm in Sub A10 and 0.99 nm in Sub B10, and 1.47 nm in Sub A30 and

1.06 nm in Sub B30, while  $R_c$  values in the monomer are 1.64 nm at 10 °C and 1.20 nm at 30 °C. These donor–acceptor distances mostly became shorter in dimer compared to those in monomer.

### Inter-subunit structure

The dynamics of distances between Iso in Sub A and Iso in Sub B are shown in Fig. S1 (ESI†). The centre-to-centre distances ( $R_c$ ) were shorter at 30 °C than at 10 °C. The distance distributions are shown in the right column. The dynamics and distributions of Iso–Iso inter-planar angles are shown in the bottom panels. The mean distances over 5000 snapshots were 4.15 nm at 10 °C and 4.09 nm at 30 °C. The mean angles were 78° at 10 °C and 85° at 30 °C.

### Root of mean square fluctuations

The root of mean square fluctuation (RMSF) is considered to be a good index for structural fluctuation of an individual amino acid, which was obtained by Amber10.<sup>38</sup> Fig. 4 shows RMSF of Sub A and Sub B at both 10 °C and 30 °C. RMSF was highest around residue No. 300 in all four systems, Arg297-Phe298-Gly299-Ser300-Ser301-Asn302-Thr303. The highest amino acids were Ser300 in Sub A10, Gly299 in Sub B10, Ser300 in Sub A30 and Gly299 in Sub B30. Next highest regions were around the residue No. 170. The peak amino acids in this region were Arg172 in Sub A10 and in Sub B10, and Gly173 in Sub A30 and Arg172 in Sub B30. The third highest RMSF were near C-terminals, Asn338 in Sub A10, Arg337 in Sub B10, Arg337 in Sub A30, and Glu336 in Sub B30. The values of RMSF were always higher at 10 °C than at 30 °C, despite that thermal fluctuation of the

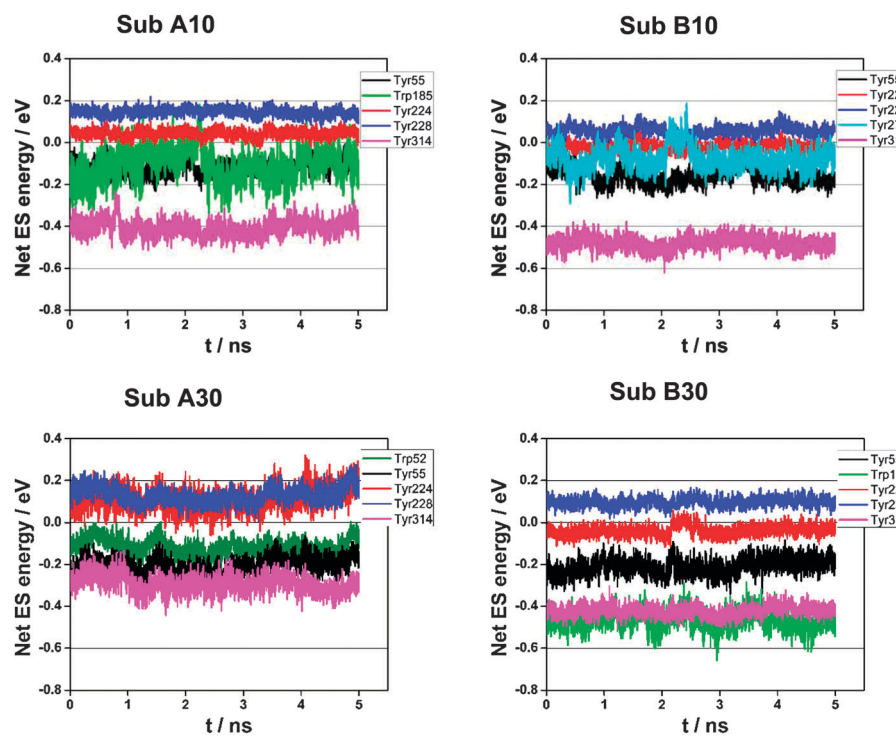


Fig. 8 Dynamics of Net ES energy in DAAO dimer. Sub A10 and Sub B10 denote Sub A and Sub B at 10 °C, and Sub A30 and Sub B30, Sub A and Sub B at 30 °C. Insets show donors with top fastest ET rates.

protein should increase with temperature. Mean RMSF over all residues were highest in Sub B10 (0.403), followed by Sub A10 (0.401), Sub A30 (0.294) and Sub B30 (0.285).

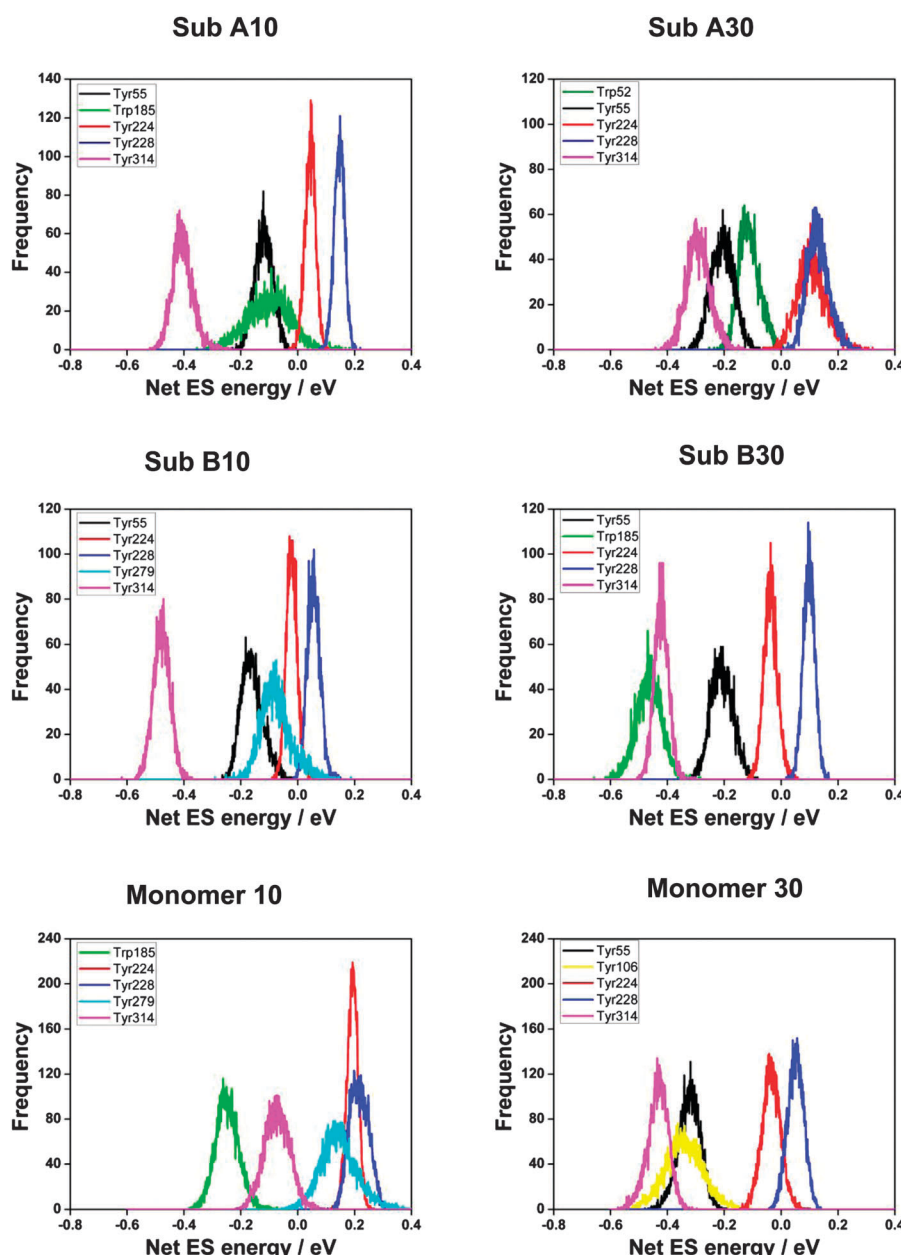
#### H-bond structure between Iso and surrounding amino acids

Fig. 5 shows the H-bond structure. Table 2 lists the mean H-bond distances (RH) over 5000 snapshots within 0.3 nm. The atom notations of the Iso ring are shown in Chart 1. In both Sub A10 and Sub B10 IsoN3H forms H-bond with Leu51O (peptide) with RH values of both 0.29 nm, but not at all in both Sub B10 and Sub B30. IsoN5 form H-bond with Ala49N (peptide) only in Sub A10 (RH 0.29 nm). IsoO2 forms H-bonds with peptide nitrogen atoms of Gly315N (RH 0.29 nm), Leu316N (RH 0.28 nm) and Thr317 (RH 0.29 nm) in

both Sub B10 and Sub B30, but not H-bonds in Sub A at both temperatures. IsoO2 in Sub A forms single H-bond with side-chain OH of Thr317 in both Sub A10 and Sub A30 (RH 0.28 nm), but not in Sub B. IsoO4 forms H-bonds with peptide nitrogen atoms of Gly50 and Leu51 only in Sub A10, but not in Sub B at both temperatures. These findings suggest that Sub A and Sub B are not equivalent at Iso binding sites.

#### ET parameters

ET parameters obtained by the method described above are listed in Table 3. The static dielectric constants inside the protein were  $\epsilon_0^A = \epsilon_0^B = 5.8$ , which were obtained assuming to be independent of temperature.<sup>36</sup> The dielectric constant for



**Fig. 9** Distributions of Net ES energy. The Net ES energies were obtained with the entire model in which contributions of the energies from both subunits are included. Insets show donors with top fastest ET rates.

Tyr224 and Tyr228 between the donors and acceptor ( $\varepsilon_0^{\text{DA}}$ ) was also 5.8, which did not change from those inside Sub A and Sub B ( $\varepsilon_0^k$ ,  $k = \text{A}$  and  $\text{B}$ ). The reason for it is discussed later. Free energies related to electron affinity of Iso\*  $\{G_k^0(T)\}$  were 8.2 eV in Sub A10 and 8.5 eV in Sub B10, and 8.7 eV in Sub A30 and 8.5 eV in Sub B30. The calculated lifetimes completely coincided with the observed lifetimes.<sup>23</sup>

#### ET rates from aromatic amino acids to Iso\*

Time evolutions of logarithmic ET rates are shown in Fig. 6. In Sub A10 the rate was fastest from Tyr224. The rate from Trp185 displayed sudden transitions at around 1 ns and 2.5 ns, which may be related to the double maxima in  $R_c$  distribution. In Sub B10 the rate was fastest from Tyr314. The fastest donors were Tyr228 in Sub A30 and Tyr314 in Sub B30. Mean ET rates over MDS snapshots (5000 with 1 ps intervals) are listed in Table 4. In Sub A10 the rates from Tyr224, Tyr314 and Tyr228 were  $1.3 \times 10^{-2}$ ,  $7.6 \times 10^{-3}$ , and  $1.2 \times 10^{-3} \text{ ps}^{-1}$ , respectively, followed by

Tyr55 and Trp185. The order of  $R_c$  in Sub A10 were Tyr224, Tyr228, Tyr55, Tyr314 and Tyr279, which were considerably different from the order in ET rates. In Sub B10, the ET rates were  $1.4 \times 10^{-2}$  from Tyr314,  $6.0 \times 10^{-3}$  from Tyr224 and  $1.5 \times 10^{-3} \text{ ps}^{-1}$  from Tyr55, followed by Tyr228 and Tyr279. The order of  $R_c$  in Sub B10 were the same with Sub A10.  $R_c$  of Tyr314 in Sub B10 was the forth shortest, but the ET rate was fastest. In Sub A30 five fastest donors were Tyr314 ( $1.6 \times 10^{-2} \text{ ps}^{-1}$ ), Tyr228 ( $5.9 \times 10^{-3} \text{ ps}^{-1}$ ), Tyr224 ( $3.5 \times 10^{-3} \text{ ps}^{-1}$ ), Tyr55 and Trp52 in this order, while the order of  $R_c$  in Sub 30A was Tyr228, Tyr224, Tyr314, Tyr279 and Tyr55. In Sub B30 they were Tyr224 ( $1.7 \times 10^{-2} \text{ ps}^{-1}$ ), Tyr314 ( $6.5 \times 10^{-3} \text{ ps}^{-1}$ ), Trp185 ( $1.4 \times 10^{-3} \text{ ps}^{-1}$ ), Tyr55 and Tyr228, while the order of  $R_c$  in Sub 30B was Tyr224, Tyr228, Tyr314, Tyr55 and Trp185.

Fig. 7 illustrates distribution of logarithmic ET rates from aromatic amino acids to Iso\*. The distribution pattern was quite different between Sub A and Sub B, and also between 10 °C and 30 °C. Half width of the distribution indicates extent

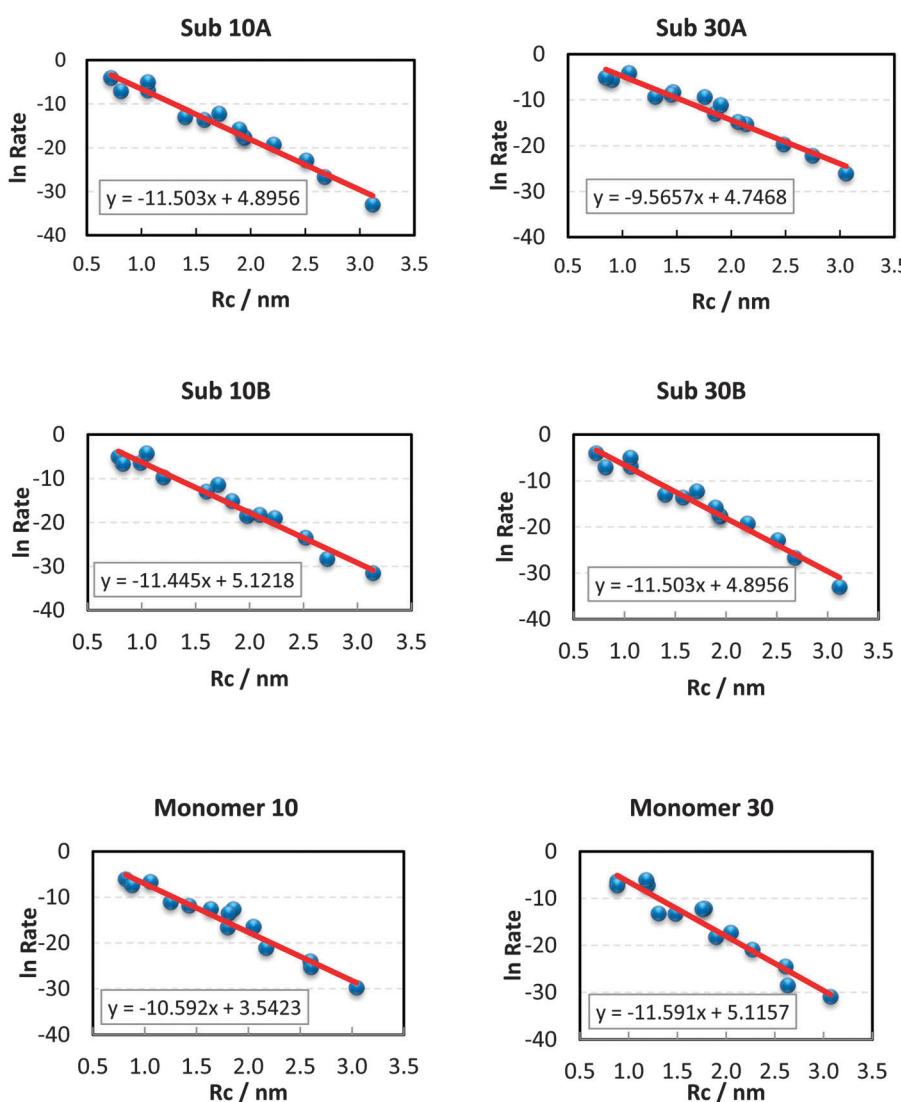


Fig. 10 Dutton law for Tyrs as ET donor in DAAO. All Tyrs were taken into account. Insets indicate approximate linear functions. Dutton law for the monomer is also shown for comparison. Absolute value of slope was least in Sub 30A in the dimer.

of fluctuation in the logarithmic rate. Most of the donors displayed marked fluctuations. The logarithmic rates from Tyr314 were relatively sharp in all cases. The distribution of Trp185 in Sub A10 displayed double maxima which should be ascribed to double maxima in  $R_c$  (see Fig. 3). ET rate from Tyr228 was the second fastest in Sub 30A, but quite slow in Sub B30. The rate from Trp185 was the third fastest in Sub B30, but much slow in the other systems.

The effects of subunit structures on the ET rates are shown in Fig. S2 (ESI†). In independent model of Fig. S2 (ESI†) the ET rates were obtained separately in Sub A and in Sub. In the entire model the ET rates were obtained for the entire dimer. The distributions of the Net ES energies obtained with the entire model were quite different from those with the independent model.

### Physical quantity related to ET rate

Fig. 8 shows dynamics of Net ES energy obtained by eqn (5). The fluctuation of the energy in Tyr224 and Tyr228 were relatively small. The energy of Trp185 in Sub A10 displayed marked fluctuation. The Net ES energy,  $E_{\text{Net}}^k(j)$ , of Tyr314 were always low ( $-0.3$  to  $-0.5$  eV), despite the ET rate were fastest or second fastest among the donors. The reason for it is discussed later. Fig. 9 shows distribution of Net ES energy. As stated above, Net ES energies of Tyr314 were always negative and very low. The Net ES energies of Tyr228 were always positive and highest among the donors with top five ET rates.

Physical quantities other than ET rate are listed in Table 4 including the Net ES energy. Solvent reorganization energy

obtained by eqn (2),  $\lambda_{jk}^q$ , did not display much variation among the donors, 1.7–2.1 eV. ES energy between Iso anion and a donor cation,  $-e^2/\epsilon_0^{pk}R_{jk}$ , varied from  $-0.17$  eV in Tyr55 of Sub A30 to  $-0.34$  eV in Tyr224 of Sub B30.

The effects of subunit structures on the Net ES energies are shown in Fig. S3 (ESI†). In the independent model of Fig. S3 (ESI†) Net ES energies were obtained separately in Sub A and in Sub. In the entire model the Net ES energies were obtained for the entire dimer. The distributions of the Net ES energies obtained with the entire model were quite different from those with the independent model. This suggests that appreciable Net ES energies from Sub B contribute to those in Sub A.

### Dutton law

According to Moser *et al.*,<sup>45</sup> logarithmic ET rate linearly decreases with the donor–acceptor distance, which is called Dutton law. In the present work Tyrs are major donors to Iso\*. Dutton law for Tyrs was examined in all Sub A10, Sub B10, Sub A30 and Sub B30. Fig. 10 shows dependence of the logarithmic ET rates for all Tyrs on  $R_c$ . In all systems the logarithmic ET rates were well approximated with linear function, which reveals that Dutton law is valid in DAAO dimer. The slopes of the straight lines were  $-11.5$  in Sub A10,  $-11.4$  in Sub B10,  $-9.6$  in Sub A30 and  $-11.5$  in Sub B30. Dutton law for DAAO monomer was also examined at  $10$  °C and  $30$  °C for comparison (see bottom of Fig. 10). The logarithmic rates of the monomer were also well described with linear functions of  $R_c$ . The slopes were  $-10.6$  at  $10$  °C and  $-11.6$  at  $30$  °C. Dutton law for all Trps

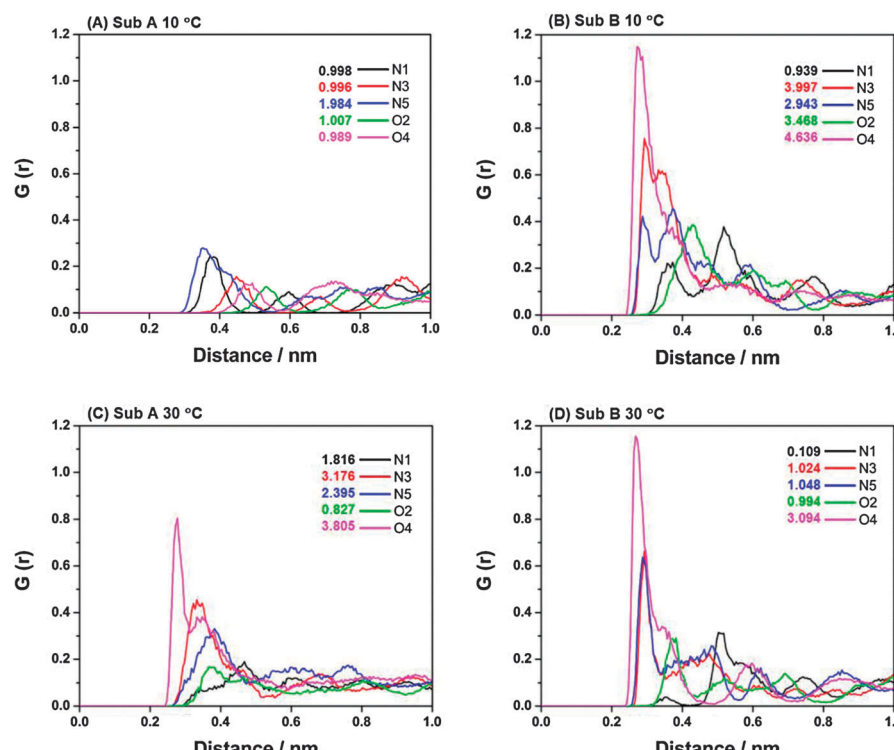


**Fig. 11** Radial distribution function derived number of water molecules near hetero atoms in Iso ring in DAAO dimer. The radial distribution functions (RDF) were obtained by *ptraj* module of Amber10 program.<sup>38</sup> Insets indicate number of mean water molecules at the distances from the hetero atoms in Iso.

is shown Fig S4 (ESI<sup>†</sup>). The logarithmic ET rates of Trps also decreased linearly with  $R_c$ . The slopes of the linear functions were 20–23, which were quite different from those of Tyr. The magnitude of the slope was least in Sub A30 as that of Tyr (see Fig. 10).

#### Energy gap law

Dependence of logarithmic ET rates on total standard free energy gap  $\{\Delta G_{\text{Total}}^0(T)\}$  is called energy gap law.  $\Delta G_{\text{Total}}^0(T)$  is obtained by eqn (8).

$$-\Delta G_{\text{Total}}^0(T) = -\{\Delta G_k^0(T) - e^2/\epsilon_0^{\text{pk}} R_{jk} + E_{\text{Net}}^k(j)\} \quad (8)$$

The quantities of the right hand side for major donors (Tyr) are given in Table 4. Fig. S5 (ESI<sup>†</sup>) shows the energy gap law of Tyr as the donors in DAAO dimer. The energy gap law of Tyr in DAAO monomer was also shown for comparison. The logarithmic rates were well approximated with parabolic functions in all systems. The insets in Fig. S5 (ESI<sup>†</sup>) represent approximate parabolic functions,  $Y = aX^2 + bX + c$ , where  $Y$  is  $\ln k_{\text{ET}}^{\text{lk}}(T)$  and  $X$ ,  $\Delta G_{\text{Total}}^0(T)$ . Fig. S5 (ESI<sup>†</sup>) reveals that ET from Tyr to Iso\* in any cases takes place in normal region. Maximum rates in the dimer were expected at 1.2 eV of  $\Delta G_{\text{Total}}^0(T)$  in Sub A10, at 1.6 eV in Sub B10, at 1.2 eV in Sub A30 and 1.8 eV in Sub

B30. The maximum rates in the monomer were expected at 0.90 eV at 10 °C and at 0.77 eV at 30 °C, which were much smaller than those in the dimer.

## IV. Discussion

Sub A and Sub B displayed quite different structures in solution. Accordingly different physical quantities related to ET were obtained in the following points; (1)  $R_{\text{cS}}$  of Tyr55, Tyr314 and Tyr279 quite shorter in Sub B10 than those in Sub A10, while  $R_c$  of Trp185 was much longer in Sub B10 (see Table 1 and Fig. 3), (2) IsoO2 formed H-bond exclusively with Thr317OG1 (side chain) in both Sub A10 and Sub A30, while it formed with Gly315N (peptide), Leu316N and Thr317N in Sub B10 and Sub B30, (3) IsoO4 formed H-bond with Gly50N and Leu51N in Sub A10, while it did not form H-bonds with any amino acids in Sub B10, (4) electron affinity of Iso\*  $\{G_k^0(T)\}$  in eqn (3) was appreciably lower in Sub A10 compared to Sub B10 (see Table 3), while static dielectric constant inside the subunits did not differ between Sub A and Sub B, (5) ET rate to Iso\* was fastest from Tyr224 in Sub A10, while it was fastest from Tyr314 in Sub B10.

The temperature transition in DAAO is also found in the dimer in fluorescence lifetimes,<sup>23</sup> though it is not so

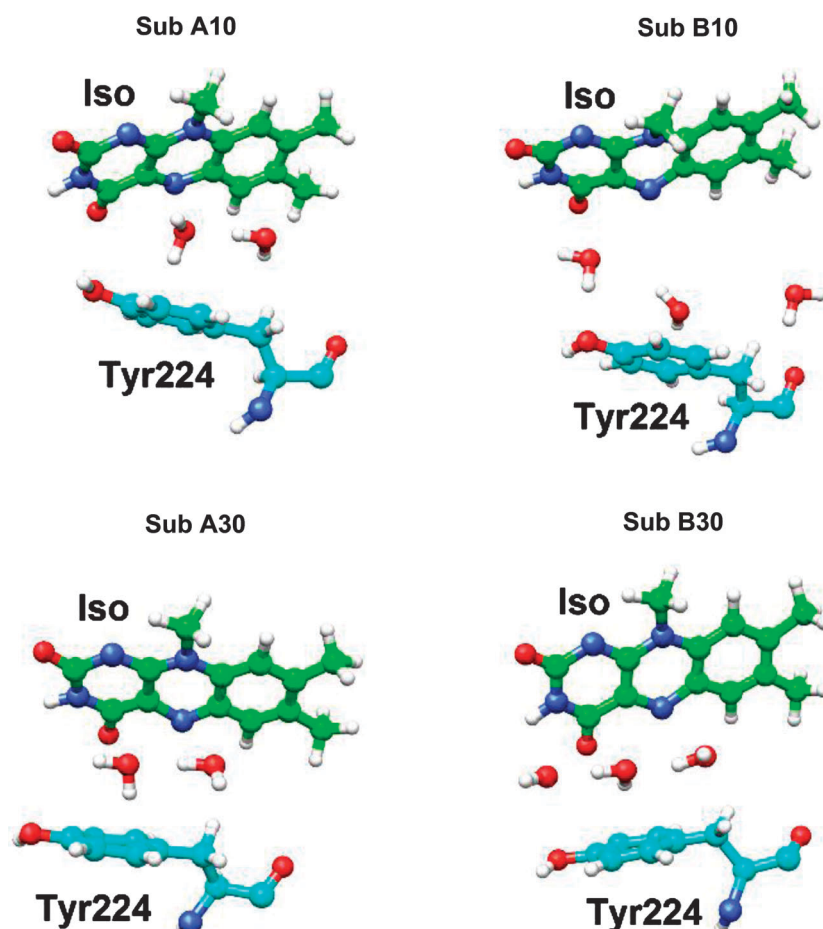


Fig. 12 Presence of water molecules between Iso and Tyr224. The structure was obtained from a snapshot in the respective category. Some times more than one water molecules and even an amino acid can come into the region between Iso and Tyr224.

pronounced as in the monomer. The structures and the physical quantities were temperature-dependent in the following points; (1)  $R_c$  (0.74 nm) of Tyr224 which was shortest in Sub A10, became much longer (0.90 nm) in Sub A30, instead,  $R_c$  of Tyr224 in Sub B10 became a little shorter (0.72 nm) in Sub B30, (2) the values of  $G_k^0(T)$ , 8.2 in Sub A10 and 8.5 eV in Sub B10, changed to 8.7 and 8.5 eV in Sub A30 and Sub B30, respectively, whereas the dielectric constant inside the protein did not depend on temperature, (3) ET rate from Tyr224 in Sub A10 reduced by 30% in Sub A30, while that of Tyr314 (second fastest in Sub A10) increased by twice in Sub A30, (4) ET rate from Tyr314 in Sub B10 which was fastest, reduced by 50% in Sub B30, while that of Tyr224 in Sub B10 increased by 3 times in Sub B30.

The fluorescence of DAAO dimer always decays with single lifetime upon changing both the protein concentration and temperature within experimental time resolution,<sup>23</sup> despite that the dimer is expected to display two-lifetime components from Sub A and Sub B if we consider the differences in the structures and physical quantities stated above. The fluorescence decays with total rate summed over the rates from all donors (see eqn (6)). The total rate did not differ appreciably between the two subunits. The fluorescence lifetimes of the monomer are around 160 ps, while it is *ca.* 40 ps in the dimer.<sup>23</sup> It is important to elucidate why the dimer has shorter lifetime than the monomer. In both DAAO dimer and monomer, Net ES energy  $\{E_{\text{Net}}^k(j)\}$  were mostly negligible compared to solvent reorganization energy ( $\lambda_{jk}^q$ ; see Table 4), which implies that the shorter lifetimes of Iso\* in dimer cannot be elucidated solely in terms of the Net ES energies. On the other hand  $R_c$  between Iso and the donors were quite shorter in dimer than those in monomer.  $R_c$  ratio in Table 4 shows the ratio,  $R_c$  (dimer)/ $R_c$  (monomer). Mostly values of the ratio were smaller than 1, which means that  $R_c$  values of major donors in dimer are shorter than those in monomer. Dutton law in DAAO reveals that the logarithmic ET rates linearly decrease with  $R_c$ . This should be main reason why the lifetimes of dimer are shorter than those of monomer.<sup>23</sup>

The static dielectric constant,  $\epsilon_0^{\text{DA}}$ , between Iso and donors (Tyr224 and Tyr228) did not change from those inside the entire subunits,  $\epsilon_0^A$  and  $\epsilon_0^B$ . This is in contrast with those of FMN binding proteins,<sup>33</sup> flavodoxin from *Helocobactor pylori*<sup>52</sup> and DAAO–benzoate complex,<sup>37</sup> where the values of  $\epsilon_0^{\text{DA}}$  were less than 3. In these protein systems  $R_c$ s between Iso and the donors are very short, and so that no amino acid or water molecule can come into the region between Iso and the donors. In contrast with it  $R_c$  between Iso and Tyr224 or Tyr228 (shortest among the donors) in DAAO were quite long and so water molecules and other amino acids can be located in this region. Fig. 11 shows radial distribution functions,  $G(r)$ , of water molecules near Iso, which were obtained with MDS snapshots. The distribution displayed sharp peaks at around 0.3 nm (first layer from hetero atoms in Iso), which shows that the presence of water molecules was quite steady. Similar situation is found in the monomer.<sup>37</sup> Fig. 12 shows presence of water molecules between Iso and Tyr224 obtained by a

snapshot of MDS. In any systems more than one water molecules locate between Iso and Tyr224. These structures may be time-dependent. In some snapshots two or more water molecules came into the region, and also nearby amino acid. These results provide molecular basis for high  $\epsilon_0^{\text{DA}}$  in DAAO dimer as in the monomer.<sup>36,37</sup>

## References

- 1 R. Miura, C. Setoyama, Y. Nishina, K. Shiga, I. Miyahara, H. Mizutani and K. Hirotsu, *J. Mol. Catal. B: Enzym.*, 2001, **12**, 43–52.
- 2 V. I. Tishkov and S. V. Khoronenkova, *Biochemistry*, 2005, **70**, 40–54.
- 3 L. Pollegioni, L. Piubelli, S. Sacchi, M. S. Pilone and G. Molla, *Cell. Mol. Life Sci.*, 2007, **64**, 1373–1394.
- 4 T. Kawazoe, H. K. Park, S. Iwana, H. Tsuge and K. Fukui, *Chem. Rec.*, 2007, **7**, 305–315.
- 5 S. Sacchi, L. Caldinelli, P. Cappelletti, L. Pollegioni and G. Molla, *Amino Acids*, 2012, **43**, 1833–1850.
- 6 C. Madeira, M. E. Freitas, C. Vargas-Lopes, H. Wolosker and R. Panizzutti, *Schizophr. Res.*, 2008, **101**, 76–83.
- 7 M. P. M. Boks, T. Rietkerk, M. H. van de Beek, I. E. Sommer, T. J. de Koning and R. S. Kahn, *Eur. Neuropsychopharmacol.*, 2007, **17**, 567–572.
- 8 M. Katane, N. Osaka, S. Matsuda, K. Maeda, T. Kawata, Y. Saitoh, M. Sekine, T. Furuchi, I. Doi, S. Hirono and H. Homma, *J. Med. Chem.*, 2013, **56**, 1894–1907.
- 9 M. L. Fonda and B. M. Anderson, *J. Biol. Chem.*, 1968, **243**, 5635–5643.
- 10 S. W. Henn and G. K. Ackers, *Biochemistry*, 1969, **8**, 3829–3838.
- 11 S. W. Henn and G. K. Ackers, *J. Biol. Chem.*, 1969, **244**, 465–470.
- 12 K. Yagi and N. Ohishi, *J. Biochem.*, 1972, **71**, 993–998.
- 13 E. Antonini, M. Brunori, M. R. Buzzesi, E. Chiancone and V. Massey, *J. Biol. Chem.*, 1966, **241**, 2358–2366.
- 14 H. Tojo, K. Horiike, K. Shiga, Y. Nishina, H. Watari and T. Yamano, *J. Biol. Chem.*, 1985, **260**, 12607–12614.
- 15 H. Tojo, K. Horiike, K. Shiga, Y. Nishina, H. Watari and T. Yamano, *J. Biol. Chem.*, 1985, **260**, 12615–12621.
- 16 H. Mizutani, I. Miyahara, K. Hirotsu, Y. Nishina, K. Shiga, C. Setoyama and R. Miura, *J. Biochem.*, 1996, **120**, 14–17.
- 17 A. Mattevi, M. A. Vanoni, F. Todone, M. Rizzi, A. Teplyakov, A. Coda, M. Bolognesi and B. Curti, *Proc. Natl. Acad. Sci. U. S. A.*, 1996, **93**, 7496–7501.
- 18 V. Massey, B. Curti and H. Ganther, *J. Biol. Chem.*, 1966, **241**, 2347–2357.
- 19 J. F. Koster and C. Veeger, *Biochim. Biophys. Acta, Enzymol.*, 1968, **167**, 48–63.
- 20 K. Shiga and T. Shiga, *Biochim. Biophys. Acta, Protein Struct.*, 1972, **263**, 294–303.
- 21 K. Yagi, F. Tanaka, N. Nakashima and K. Yoshihara, *J. Biol. Chem.*, 1983, **258**, 3799–3802.
- 22 F. Tanaka, N. Tamai and I. Yamazaki, *Biochemistry*, 1989, **28**, 4259–4262.

- 23 F. Tanaka, N. Tamai, I. Yamazaki, N. Nakashima and K. Yoshihara, *Biophys. J.*, 1989, **56**, 901–909.
- 24 A. Karen, N. Ikeda, N. Mataga and F. Tanaka, *Photochem. Photobiol.*, 1983, **37**, 495–502.
- 25 A. Karen, M. T. Sawada, F. Tanaka and N. Mataga, *Photochem. Photobiol.*, 1987, **45**, 49–53.
- 26 D. Zhong and A. H. Zewail, *Proc. Natl. Acad. Sci. U. S. A.*, 2001, **98**, 11867–11872.
- 27 N. Mataga, H. Chosrowjan, Y. Shibata, F. Tanaka, Y. Nishina and K. Shiga, *J. Phys. Chem. B*, 2000, **104**, 10667–10677.
- 28 N. Mataga, H. Chosrowjan, S. Taniguchi, F. Tanaka, N. Kido and M. Kitamura, *J. Phys. Chem. B*, 2002, **106**, 8917–8920.
- 29 H. Chosrowjan, S. Taniguchi, N. Mataga, F. Tanaka, D. Todoroki and M. Kitamura, *J. Phys. Chem. B*, 2007, **111**, 8695–8697.
- 30 H. Chosrowjan, S. Taniguchi, N. Mataga, F. Tanaka, D. Todoroki and M. Kitamura, *Chem. Phys. Lett.*, 2008, **462**, 121–124.
- 31 H. Chosrowjan, S. Taniguchi, N. Mataga, T. Nakanishi, Y. Haruyama, S. Sato, M. Kitamura and F. Tanaka, *J. Phys. Chem. B*, 2010, **114**, 6175–6182.
- 32 N. Nunthaboot, F. Tanaka, S. Kokpol, H. Chosrowjan, S. Taniguchi and N. Mataga, *J. Phys. Chem. B*, 2008, **112**, 13121–13127.
- 33 N. Nunthaboot, S. Pianwanit, S. Kokpol and F. Tanaka, *Phys. Chem. Chem. Phys.*, 2011, **13**, 6085–6097.
- 34 K. Lugsangangarm, S. Pianwanit, S. Kokpol, F. Tanaka, H. Chosrowjan, S. Taniguchi and N. Mataga, *J. Photochem. Photobiol. A*, 2011, **219**, 32–41.
- 35 N. Nunthaboot, N. Kido, F. Tanaka, K. Lugsangangarm, A. Nueangaudom, S. Pianwanit and S. Kokpol, *J. Photochem. Photobiol. A*, 2013, **252**, 14–24.
- 36 A. Nueangaudom, K. Lugsangangarm, S. Pianwanit, S. Kokpol, N. Nunthaboot and F. Tanaka, *Phys. Chem. Chem. Phys.*, 2012, **14**, 2567–2578.
- 37 A. Nueangaudom, K. Lugsangangarm, S. Pianwanit, S. Kokpol, N. Nunthaboot and F. Tanaka, *J. Photochem. Photobiol. A*, 2012, **250**, 6–17.
- 38 D. A. Case, T. A. Darden, I. T. E. Cheatham, C. L. Simmerling, J. Wang, R. E. Duke, R. Luo, M. Crowley, R. C. Walker, W. Zhang, K. M. Merz, B. Wang, S. Hayik, A. Roitberg, G. Seabra, I. Kolossváry, K. F. Wong, F. Paesani, J. Vanicek, X. Wu, S. R. Brozell, T. Steinbrecher, H. Gohlke, L. Yang, C. Tan, J. Mongan, V. Hornak, G. Cui, D. H. Mathews, M. G. Seetin, C. Sagui, V. Babin and P. A. Kollman, *AMBER 10*, University of California, San Francisco, 2008.
- 39 J. Wang, P. Cieplak and P. A. Kollman, *J. Comput. Chem.*, 2000, **21**, 1049–1074.
- 40 C. I. Bayly, P. Cieplak, W. Cornell and P. A. Kollman, *J. Phys. Chem.*, 1993, **97**, 10269–10280.
- 41 U. Essmann, L. Perera, M. L. Berkowitz, T. Darden, H. Lee and L. G. Pedersen, *J. Chem. Phys.*, 1995, **103**, 8577–8593.
- 42 J.-P. Ryckaert, G. Ciccotti and H. J. C. Berendsen, *J. Comput. Phys.*, 1977, **23**, 327–341.
- 43 R. A. Marcus, *J. Chem. Phys.*, 1956, **24**, 966–978.
- 44 R. A. Marcus, *Annu. Rev. Phys. Chem.*, 1964, **15**, 155–196.
- 45 C. C. Moser, J. M. Keske, K. Warncke, R. S. Farid and P. L. Dutton, *Nature*, 1992, **355**, 796–802.
- 46 T. Kakitani and N. Mataga, *J. Phys. Chem.*, 1985, **89**, 8–10.
- 47 A. Yoshimori, T. Kakitani, Y. Enomoto and N. Mataga, *J. Phys. Chem.*, 1989, **93**, 8316–8323.
- 48 N. Matsuda, T. Kakitani, T. Denda and N. Mataga, *Chem. Phys.*, 1995, **190**, 83–95.
- 49 F. Tanaka, H. Chosrowjan, S. Taniguchi, N. Mataga, K. Sato, Y. Nishina and K. Shiga, *J. Phys. Chem. B*, 2007, **111**, 5694–5699.
- 50 F. Tanaka, R. Rujkorakarn, H. Chosrowjan, S. Taniguchi and N. Mataga, *Chem. Phys.*, 2008, **348**, 237–241.
- 51 V. Vorsa, T. Kono, K. F. Willey and N. Winograd, *J. Phys. Chem. B*, 1999, **103**, 7889–7895.
- 52 K. Lugsangangarm, S. Pianwanit, A. Nueangaudom, S. Kokpol, F. Tanaka, N. Nunthaboot, K. Ogino, R. Takagi, T. Nakanishi, M. Kitamura, S. Taniguchi and H. Chosrowjan, *J. Photochem. Photobiol. A*, 2013, **268**, 58–66.